ISBN: 978-3-95450-253-0 ISSN: 2673-5571 doi:10.18429/JACoW-HB2023-WEA4I1

# DEVELOPMENT OF NON-DESTRUCTIVE BEAM ENVELOPE MEASUREMENTS USING BPMs FOR LOW-BETA HEAVY ION BEAMS IN SRF CAVITIES

T. Nishi*, T. Adachi, O. Kamigaito, N. Sakamoto, T. Watanabe, K. Yamada
RIKEN Nishina Center, Wako, Saitama, Japan

*Abstract*

Accurate measurement and control of the beam envelope are crucial issues, particularly in high-power accelerator facilities. However, the use of destructive monitors is limited to low-intensity beams. Furthermore, in the case of beam transport between superconducting cavities, these destructive monitors should be avoided to prevent the generation of dust particles and outgassing. In the Superconducting RIKEN LINAC, or SRILAC, we utilize eight non-destructive Beam Energy Position Monitors (BEPMs)to measure beam positions and energies. Currently we are developing a method to estimate the beam envelope by combining the quadrupole moments from BEPMs, which consist of four cosine-shape electrodes, with transfer matricesWhile this method has been applied to electron and proton beams, it has not been practically demonstrated for heavy ion beams in $\beta \simeq 0.1$ regions. By combining BEPM simulations, we are making progress toward the reproduction of experimental results, overcoming specific issues associated with low $\beta$. This development will present the possibility of a new method for beam envelope measurement in LEBT and MEBT, especially for hadron beam facilities.

## INTRODUCTION: SRILAC AND BEPMS

The Superconducting RIKEN LINAC, or SRILAC [1], started operation in 2020, and it has been providing a stable supply of heavy ion beam with intensity of a few pμA and beam energy of about 6 MeV/u [1, 2]. In the future, the intensity is planned to increase up to 10 pμA. SRILAC will be also used for medical isotope production as well as an injector for the RI beam factory, where higher beam intensities are required. Precise measurement and control of the beam dynamics are essential to achieve stable operation in high-intensity conditions. However, to suppress dust production and outgassing there are no destructive monitors between Superconducting RF (SRF) cavities. The only option to optimize the beam envelope inside the cavities was to minimize the vacuum levels between cavities. To estimate the beam dynamics in these sections, we performed Q-scan measurement downstream, changing the magnetic field of quadrupole magnets several times and measuring the beam profile for each magnetic field to reconstruct the phase ellipse [3]. Based on the obtained phase ellipse downstream of SRF cavities, we can estimate the beam envelope with transfer matrices [4] from the cavity sections to downstream sections. A disadvantage of the Q-scan method is that we cannot perform the measurement frequently during beam supply to the users because it takes at least 30 minutes and we need to temporary change the magnetic fields. Another restriction of the method is to decrease the beam intensity down to $\simeq$ 100 enA to avoid melting the wire and generating dust. Therefore, we started to develop an improved beam envelope measurement method using non-destructive monitors Beam Energy Position Monitors (BEPMs) [5].

Figure 1 shows the layout of SRILAC and beamline with eight BEPMs in between SRF cavities. There are two types of BEPMs: type-A (numbers 1 to 6) with a longitudinal length of 50 mm and type-B (numbers 7 and 8) with a longitudinal length of 60 mm. These detectors were originally introduced to measure beam position and energy and have contributed significantly to the stable beam operation of SRILAC. The beam energy is calculated by measuring the time of flight from the time difference between signals in pairs of each section. Figure 2 shows the CAD model of type-A BEPMs on CST simulation. These BEPMs have cosine-like shape electrodes. This shape realizes the ideal response of the quadrupole moment while maintaining good linear position sensitivity [5, 6].

## PRINCIPLE TO MEASURE BEAM ENVELOPES USING BPMS

Methods for estimating beam emittance from BPM have been studied in past decades [4,7–10]. In order to understand the principle of the method, we initiate the expansion of the induced voltage of electrodes $V_{L,R,U,D}$ using transverse beam multipole moments such as the dipole ($D_{x,y}$ / $\langle x \rangle$, $\langle y \rangle$), quadrupole ($M_2$ / $\langle x^2 \rangle - \langle y^2 \rangle$ ), and higher order moment ($M_{ix,y}$, $i = 3, 4, \cdots$) [9, 10] as

$$\begin{aligned} V_R &= I_{\mathrm{beam}}(c_0 + c_1 D_x + c_2 M_2 + c_3 M_{3,x} + \cdots) \\ V_L &= I_{\mathrm{beam}}(c_0 - c_1 D_x + c_2 M_2 - c_3 M_{3,x} + \cdots) \\ V_U &= I_{\mathrm{beam}}(c_0 + c_1 D_y - c_2 M_2 + c_3 M_{3,y} + \cdots) \\ V_D &= I_{\mathrm{beam}}(c_0 - c_1 D_y - c_2 M_2 - c_3 M_{3,y} + \cdots), \end{aligned} \quad (1)$$

where $I_{\mathrm{beam}}$ denotes beam intensity and $c_i$ denotes coefficient of each multipole term. By neglecting the higher order terms from this equation, $D_{x,y}$ and $M_2$ can be obtained as

* takahiro.nishi@riken.jp

ISBN: 978-3-95450-253-0 ISSN: 2673-5571 doi:10.18429/JACoW-HB2023-WEA4I1

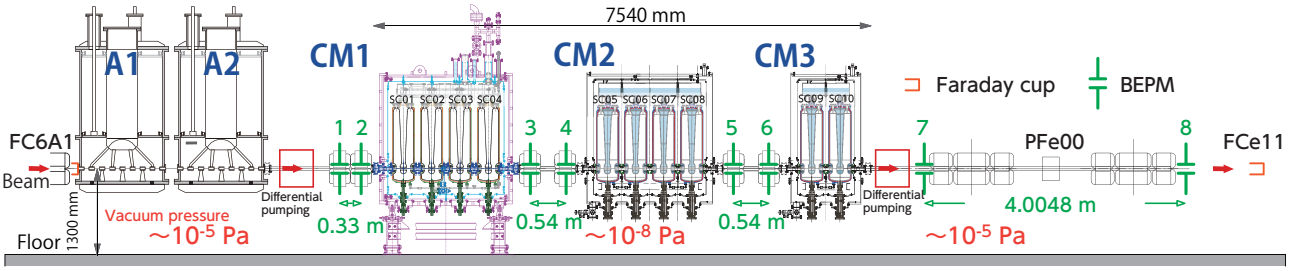


Figure 1: Schematic of beamline including SRILAC. Green numbers denote Beam Energy Position monitors, and PFe00 denotes a wire scanner.

follows,

$$D_x = \langle x \rangle = k_x \frac{V_R - V_L}{V_L + V_R + V_U + V_D}, \quad (2)$$

$$D_y = \langle y \rangle = k_y \frac{V_U - V_D}{V_L + V_R + V_U + V_D}, \quad (3)$$

$$M_2 = \langle x^2 \rangle - \langle y^2 \rangle = k_q \frac{V_R + V_L - V_U - V_D}{V_L + V_R + V_U + V_D}. \quad (4)$$

where $k_x$, $k_y$ and $k_q$ correspond to $c_1/2c_0$ and $c_2/c_0$ in Eq. (1), respectively. For the following analysis, we define $Q \equiv M_2 - D_x^2 + D_y^2 = \sigma_x^2 - \sigma_y^2$. These values are derived from the BPM signals as Eqs. (2-4). These values are also obtained from the $\sigma$ matrix of the beam at a point and the transfer matrix from that point to the BPM locations. In our beamline, $Q$ values obtained from eight BPMs and $\sigma$ matrix upstream of SRILAC can be connected via a matrix as

$$\begin{pmatrix} Q_1 \\ Q_2 \\ \vdots \\ Q_8 \end{pmatrix} = (\mathbf{H}, \mathbf{V}) \begin{pmatrix} \sigma_{xx}(0) \\ \sigma_{xx'}(0) \\ \sigma_{x'x'}(0) \\ \sigma_{yy}(0) \\ \sigma_{yy'}(0) \\ \sigma_{y'y'}(0) \end{pmatrix} \quad (5)$$

where

$$\mathbf{H} \equiv \begin{pmatrix} (M_{11}^{01})^2, 2M_{11}^{01}M_{12}^{01}, (M_{12}^{01})^2 \\ \vdots \\ (M_{11}^{08})^2, 2M_{11}^{08}M_{12}^{08}, (M_{12}^{08})^2 \end{pmatrix}, \quad (6)$$

$$\mathbf{V} \equiv \begin{pmatrix} -(M_{33}^{01})^2, -2M_{33}^{01}M_{34}^{01}, -(M_{34}^{01})^2 \\ \vdots \\ -(M_{33}^{08})^2, -2M_{33}^{08}M_{34}^{08}, -(M_{34}^{08})^2 \end{pmatrix}. \quad (7)$$

In these equations, $\sigma(0)$ indicates the elements of the $\sigma$ matrix of the beam at the upstream position denoted as 0, and $M_{ij}^{0n}$ is the $(i, j)$-th element of the transfer matrix from position 0 to the position of the $n$-th BEPM. The transfer matrices are calculated by using the beam dynamics simulation software TraceWin. The simulation with TraceWin has been able to reproduce the beam energy response to changes in phase and voltage of each cavity at a level of 0.2% and also is expected to reproduce the realistic beam dynamics, including transfer matrices. Note that the beam envelope analysis utilizes first-order transfer matrices and does not account for nonlinear effects such as space-charge effects. It is expected that the space-charge effect is sufficiently small under our beam conditions.

## BIAS ON MEASUREMENT OF QUADRUPOLE MOMENT

Using this method, we first compared the quadrupole moments variation during Q-scan measurements, as mentioned in Ref. [3]. While data showed clear positive correlations, there was also an offset between the measured values of the $Q$ moments and those estimated with Q-scan. For investigation of the underlying cause, detailed simulations were conducted using CST Studio. Figure 3 shows the comparison of waveform signals from BEPM 7 (circles) and CST calculations (lines). For the simulations, the scaling factor and timing offset are tuned to reproduce the upstream signals. In these simulations, the particle beam has no transverse emittances, i.e., $\sigma_x = \sigma_y = 0$. Despite the conditions, the peak of the signal from the downstream electrode is smaller

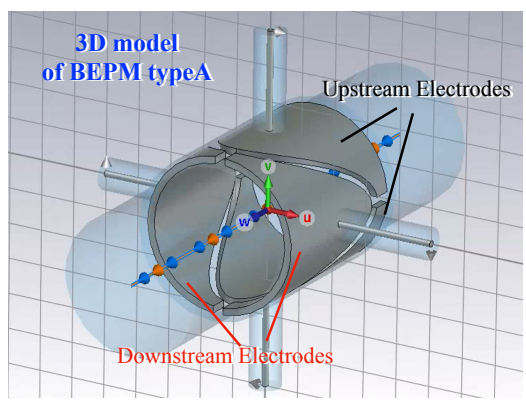


Figure 2: CAD model of type-A BEPM. The beam comes from the upper right corner towards the foreground. Up and down (right and left) electrodes are represented as upstream (downstream).

ISBN: 978-3-95450-253-0 ISSN: 2673-5571 doi:10.18429/JACoW-HB2023-WEA4I1



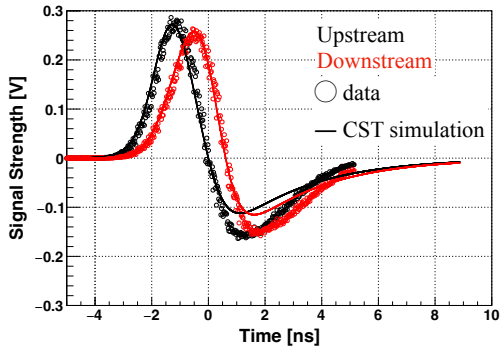


Figure 3: Waveform of the signals from BEPM electrodes. Black and red points correspond to upstream and downstream data, respectively. The lines represent the CST simulation result with the corresponding data color.

than that from the upstream electrode. A similar tendency is shown in the measured data.

The result indicates this "bias" effect should be solved in the quadrupole moment calculation based on Eq. (5) to estimate phase ellipses accurately. This effect can be qualitatively understood as follows. When considering a cylindrical BEPM, if an electrode coverage angle $\phi$, the signal voltage V of that electrode is represented as a function of time t as

$$V(\phi,t) = \mathrm{Re}\left[\Sigma_{n=0}^{\infty} \frac{jn\omega_0 R}{1+jn\omega_0 RC}\frac{\phi L I_0}{\pi\beta c}\exp\left(\frac{n^2\omega_0^2\sigma_t^2}{2}+jn\omega_0 t\right)\right]. \quad (8)$$

$R$ and $C$ represent the resistance and the capacitance of the equivalent circuit of electrodes, and $L$ is the longitudinal length of the electrodes. $\beta$, $\omega_0$, and $\sigma_t$ denote velocity, angular velocity, and time widths of the beam, respectively. To account for the shape of the electrode, the electrode is divided longitudinally by $\delta l$ and l-dependence of $\phi$ is incorporated as follows,

$$V(t) = \frac{1}{L}\int_{-L/2}^{L/2}\left\{\frac{\phi(l)}{\bar{\phi}}V\left(t-1/\beta c\right)\right\}dl. \quad (9)$$

In the equation, $\bar{\phi}$ means an averaged coverage angle of the electrode. For cosine shape BEPMs, upstream and downstream electrodes have coverages of $\phi(l) = \arccos(2l/L)$ and $\arccos(-2l/L)$, respectively.

In the case of the upstream electrode, a large signal is generated corresponding to a large $\phi$, followed by gradually overlapping signals corresponding to smaller $\phi$ with a time delay. The peak maximum is mainly determined by the signal from the upstream portion of the electrode where $\phi$ is large. On the other hand, for the downstream electrode, a relatively small signal is generated corresponding to small $\phi$, followed by gradually overlapping signals corresponding to larger $\phi$ with a time delay. In the latter case, although the peak maximum is generated by the larger $\phi$ portion of the downstream electrode, the undershoot of the signal from the upstream portion overlaps, resulting in a relatively smaller peak than that of the upstream electrode. The effect is expected to be significant when beam bunch length $\sigma_z$ is comparable to or smaller compared with the longitudinal length of the electrode. In consideration of the realistic beam bunch length in time dimension, this effect becomes significant especially for low $\beta$ particles. According to the CST simulation with beam bunch length $\sigma_t$ = 0.5 ns, the deviation of the signal strength is tiny, 0.2%, for $\beta$ = 0.99, which corresponds to the case for electron beamlines. In our case, the deviation becomes non-negligible, 5%, for $\beta$ = 0.1.

## APPLICATION FOR PHASE ELLIPSE MEASUREMENT

One possible solution is to evaluate and correct this bias effect. Application of this method is shown in Ref. [11] and has been succeeded in one-day data. However, this method requires to estimate the correction factor from experimental data beforehand. This might cause the systematic errors depending on the data with certain beam condition used for the factor estimation.

After detailed investigation, we found an alternative solution which utilizes double-integrated signals. As explained above, the origin of the bias effect lies in the time difference of signals coming from different positions of the electrodes. Integrating the signals can cancel out this effect. In fact, analysis based on CST simulations showed that the bias effect was already reduced to 1% or less with integrated signals, and eliminated for any beam bunch with double-integrated signals [12]. Consequently, we decided to adopt double integration method to experimental data. Figure 4 shows the raw, integrated, and double integrated waveform signals. For integration, the background slope caused by the offset of raw waveform signals is subtracted from the integrated waveform signals. This slope is determined to satisfy cyclic boundary conditions and ensure that the integrated signal is zero in regions (8±2 ns before the peak / shown in the figure with lines) without signals from beam. Because the obtained signals are followed by the reflected signals, we adopt the maximum of the double-integrated signals to calculate $Q$. Left bottom panel of Fig. 4 shows the measured $Q$s based on raw, integrated, and double integrated waveform signals for

Table 1: Phase Ellipse Fitting Result

| Method | $\epsilon_h$ | $\epsilon_v$ | $\alpha_h$ | $\beta_h$ | $\alpha_v$ | $\beta_v$ | $\chi^2/n.d.f.$ |
|---|---|---|---|---|---|---|---|
| Q-scan | 7.2 | 7.5 | -0.29 | 0.36 | -1.45 | 0.34 | – |
| BEPM (raw) | 3.2 | 0 | -4.0 | 1.9 | – | – | 115.7/2 |
| BEPM (bias correction) | 3.2 | 7.1 | -0.14 | 0.15 | -0.74 | 0.28 | 3.6/2 |
| BEPM (double integral) | 0.1 | 6.2 | 13.1 | 1.11 | -0.92 | 0.24 | 8.7/2 |
| BEPM $\epsilon_{h,v}$ fixed (double integral) | 7.2 | 7.5 | -0.54 | 0.60 | -1.27 | 0.33 | 14.6/4 |
| BEPM+PF (double integral) | 5.1 | 6.2 | -0.25 | 0.39 | -1.16 | 0.28 | 11.5/4 |

ISBN: 978-3-95450-253-0 ISSN: 2673-5571 doi:10.18429/JACoW-HB2023-WEA4I1

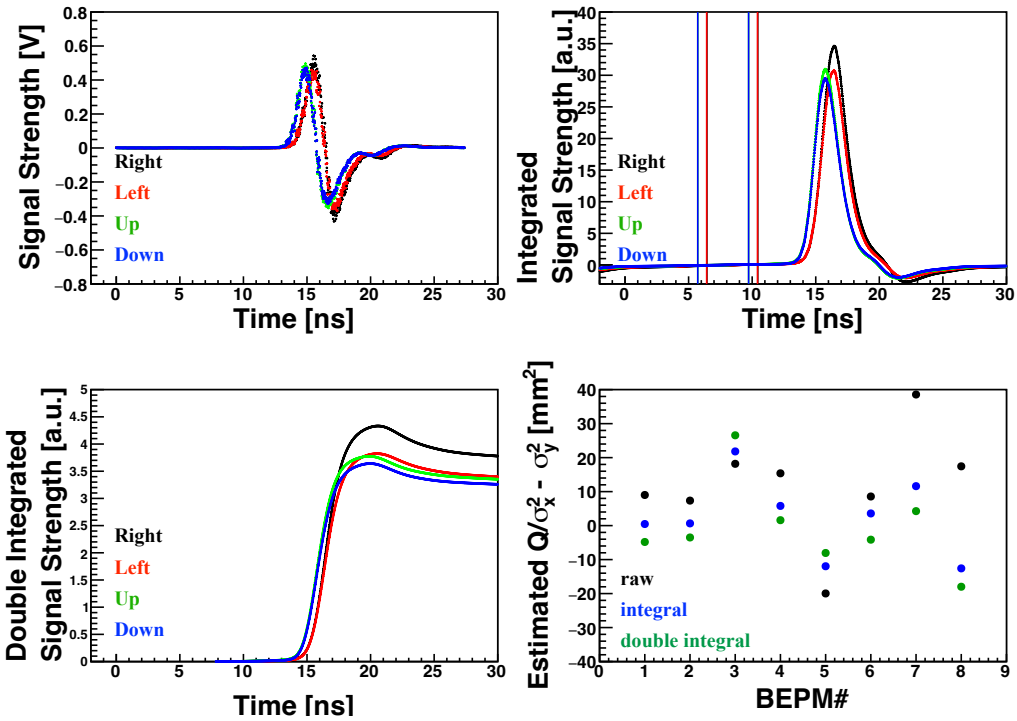


Figure 4: (Left Top) BEPM raw wave form signals from right, left, up, down electrodes. (Right Top) Integrated wave form signals after slope corrections. See the detail about the corrections in the text. (Left Bottom) Double integrated wave form signals. (Right Bottom) Measured $Q$ values of eight BEPMs based on raw, integrated, and double integrated wave form signals.

eight BEPMs. As shown, adopting integral / double-integral signals change the values of $Q$ dramatically.

With the double-integrated signals we solved the equation and estimated the $\sigma$ matrix and the phase ellipses as summarized in Table 1. As a result, the fitting chi-square significantly improved, and the fitting results well reproduced the measured $Q$ values as shown in Fig. 5 with purple circles. However, the estimated emittances were quite small and differed significantly from the results of the Q-scan, and this was also the case with the bias correction method. In contrast, when the emittance was fixed to match the results of the Q-scan, the fitting results accurately reproduced the obtained $Q$s. These results suggest inherently low sensitivity of the quadrupole moment, $\sigma_x^2 - \sigma_y^2$ to the absolute beam size.

To increase the sensitivity to the absolute beam size and make this method more practical, we attempted to implement two improvements. The first one involves imposing constraints on the emittance balance. As indicated in the table, the analysis based on the original BEPM before the improvement showed significant imbalance between the horizontal and vertical emittances, which is not realistic. Therefore, we decided to introduce a variable $\epsilon_{asym} \equiv (\epsilon_h - \epsilon_v)/(\epsilon_h + \epsilon_v)$ to represent this imbalance and impose constraints as $|\epsilon_{asym}| < 0.1$. This constrains corresponds to the deviation of $\epsilon$ of horizontal and vertical less than 20%. The second improvement is to utilize the $\sigma_x$ and $\sigma_y$ measured by the wire scanner,

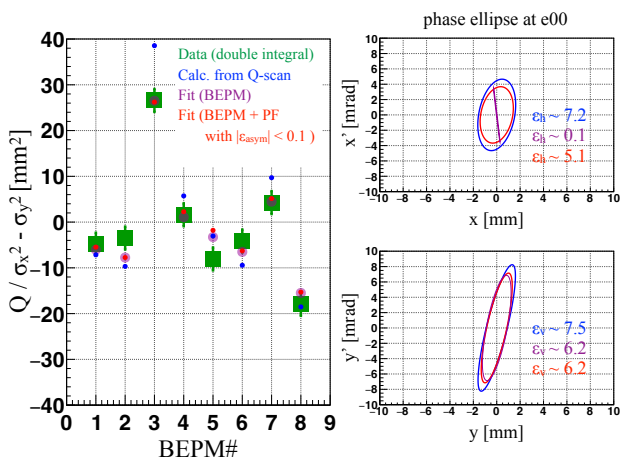


Figure 5: (Left)Q values for each BEPM based on double-integrated waveform signals. The fitting results obtained from each method are overlaid. In the analysis, errors of $Q$ values are fixed to be 2.5 mm$^2$, which is roughly estimated from the fluctuation of $Q$ measurement by BEPMs. (Right) Horizontal and vertical phase ellipses estimated by each method.

ISBN: 978-3-95450-253-0 ISSN: 2673-5571 doi:10.18429/JACoW-HB2023-WEA4I1



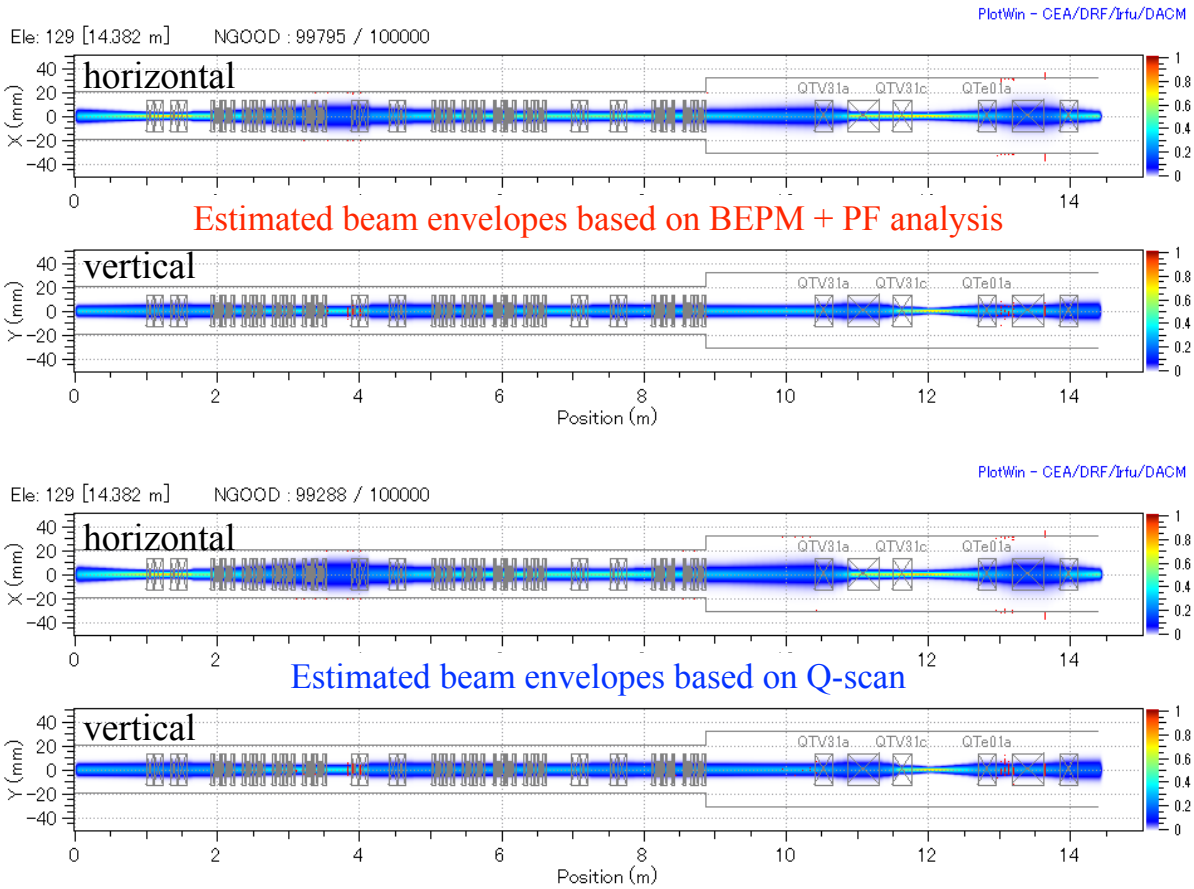


Figure 6: Estimated beam envelopes in horizontal and vertical plane through SRILAC. The envelope was calculated using TraceWin, based on the phase ellipses obtained through the analysis of BEPM + PF (Top) and Q-scan data (Bottom).

so called profile monitor or PF, located at e00 in Fig. 1. Additional information of absolute beam size is expected to improve the sensitivity for absolute value of the beam emittances.

The results of these improvements are summarized in the last column in Table 1 and in Fig. 5. As shown in the left panel of the figure, $Q$ values with and without profile monitor (PF) data show a tiny difference. However, the estimated twiss parameters and phase ellipses show large differences between these analyses. Compared with the phase ellipses estimated by Q-scan method, the fitting result with BEPM and PF data, under restriction of the $\epsilon_{asym}$, shows slightly smaller emittances and similar twiss parameters.

We also calculated beam envelopes using TraceWin, as depicted in Fig. 6. The beam envelope estimated through the BEPM + PF analysis exhibited remarkably similar results to those obtained from the Q-scan. These estimated envelopes are valuable for deducing beam loss and monitoring changes in beam conditions. While this method is no longer a truly non-destructive beam monitor, it only requires one-shot profiles with the current optics settings, making it suitable for use as a daily "semi" non-destructive beam envelope monitor. In contrast, the conventional Q-scan method necessitates changing optics settings multiple times, which is not feasible during beam supply for users.

## CONCLUSION AND FUTURE PERSPECTIVES

For the transverse beam envelope estimation in superconducting RF cavities, we have developed an improved approach utilizing BEPM signals. Despite the method's recognition over several decades, we discovered that bias effects, which is emerge with short bunch lengths or low-beta particles and the co-sin-shaped electrodes of BPM, are crucial for estimating $\sigma_x^2 - \sigma_y^2$ of the beams. By utilizing double-integrated signals, additional information from wire scanners, and applying fitting restrictions, we are able to successfully reproduce the phase ellipse observed in the Q-scan method with wire scanners. To further validate the accuracy and optimize of this approach, we plan to collect additional data and integrate it into our daily operations, with the goal of achieving more precise beam tuning. In parallel, we plan to explore the possibility of estimating the beam envelope without relying on information from devices such as wire scanners, using, for example, appropriate lattice and a sufficient number of BPMs.

ISBN: 978-3-95450-253-0 ISSN: 2673-5571 doi:10.18429/JACoW-HB2023-WEA4I1

## ACKNOWLEDGMENTS

We thank Prof. Toyama for the discussion about the method with BPMs, and our colleague Dr. Fukunishi for the discussion in the early stage of the development. We are also grateful to all operation staff for SRILAC, who help us perform all kind of measurements for the development.

## REFERENCES

[1] K. Yamada *et al.*, "Successful Beam Commissioning of Heavy-Ion Superconducting Linac at RIKEN", in *Proc. SRF'21*, East Lansing, MI, USA, Jun.–Jul. 2021, paper MOOFAV01, pp.167–174, 2021. doi:10.18429/JACoW-SRF2021-MOOFAV01

[2] H. Sakai, H. Haba, K. Morimoto, and N. Sakamoto, "Facility upgrade for superheavy-element research at RIKEN", *Eur. Phys. J. A*, vol. 58, pp. 1–15, 2022. doi:10.1140/epja/s10050-022-00888-3

[3] T. Nishi *et al.*, "Beam Acceleration with the Upgraded RIKEN Heavy-Ion Linac", in *Proc. HB'21*, Batavia, IL, USA, Oct. 2021, paper THBC1, pp. 231–234, 2021. doi:10.18429/JACoW-HB2021-THBC1

[4] R. H. Miller, J. E. Clendenin, M. B. James, and J. C. Sheppard, "Nonintercepting Emittance Monitor", in *Proc. HEACC'83*, Fermilab, IL, USA, pp. 603-605, 1983. doi:AC03-76SF00515

[5] T. Watanabe *et al.*, "Commissioning of the Beam Energy Position Monitor System for the Superconducting RIKEN Heavy-ion Linac", in *Proc. IBIC'20*, Santos, Brazil, Sep. 2020, paper FRAO04, pp. 295–302, 2020. doi:10.18429/JACoW-IBIC2020-FRAO04

[6] G. Nassibian,"The measurement of the multipole coefficients of a cylindrical charge distribution", CERN-SI-NOTE-EL-70-13, 1970, http://cds.cern.ch/record/358718/

[7] T. Suwada, K. Furukawa, and M. Satoh, "Development of a New Beam-Energy-Spread Monitor Using Multi-Stripline Electrodes", in *Proc. PAC'03*, Portland, OR, USA, May 2003, paper ROAB012, pp. 533–535, 2003. doi:10.1109/PAC.2003.1288969

[8] M. Tajima, T. Koseki, T. Nakaya, and T. Toyama, "Development of 16 Electrodes Beam-size Monitors for J-PARC MR", in *Proc. IBIC'19*, Malmö, Sweden, Sep. 2019, paper TUPP021, pp. 347–350, 2019. doi:10.18429/JACoW-IBIC2019-TUPP021

[9] T. Toyama, M. Tejima, H. Kuboki, and K. Satou, "Measurement of Transverse Dipole and Quadrupole Moments with the BPMS In the J-PARC 3-50 BT"in *Proc. IPAC'18*, Vancouver, BC, Canada, pp. 2197-2199, 2018. doi:10.18429/JACoW-IPAC2018-WEPAL020

[10] A. Sounas *et al.*, "Beam Size Measurements Based on Movable Quadrupolar Pick-ups"in *Proc. IPAC'18*, Vancouver, BC, Canada, pp. 2028-2031, 2018. doi:10.18429/JACoW-IPAC2018-WEPAF080

[11] T. Nishi, T. Adachi, O. Kamigaito, N. Sakamoto, T. Watanabe, and K. Yamada, "Development of Non-Destructive Beam Envelope Measurements in SRILAC with Low Beta Heavy Ion Beams Using BPMs", in *Proc. SRF'23*, Michigan, USA, Jun. 2023, paper MOPMB086, pp. 314–318, 2023. doi:10.18429/JACoW-SRF2023-MOPMB086

[12] T. Adachi, T. Watanabe, T. Nishi, and O. Kamigaito, "Design Study of Beam Position Monitor For Heavy-Ion Beam", in *Proc. PASJ'23*, Chiba, Japan, Aug. 2023, paper TAOA4, 2023.